Distributed Wind Power Resources for Enhanced Power Grid Resilience

Jinshun Su*, Payman Dehghanian†, Mostafa Nazemi‡ and Bo Wang§
Department of Electrical and Computer Engineering
The George Washington University
800 22nd St NW, Washington, Suite 5900, DC 20052, USA.
{*jsu66, †payman, ‡mostafa_nazemi, §wangbo}@gwu.edu

***Abstract*—Electricity outages and large scale blackouts due to natural disasters have been observed commonplace recently. Therefore, it is urgently needed to develop an efficient restoration strategy to ameliorate a grid-scale capability for restoration. With increasing penetration of renewable energy resources, it is a great potential to include wind power into the system restoration planing processes. This paper develops an efficient restoration strategy considering wind energy participation to achieve an enhanced grid resilience in response to widespread emergencies. The proposed strategy is formulated as a mixed-integer linear programming (MILP) model. In order to verify the applicability of the proposed method, the vulnerability of power elements is taken into account following a high-impact low-probability (HILP) event. The developed strategy is comprehensively tested on the modified IEEE 118-bus test system and the numerical results illustrate the efficiency of the proposed method.**

***Index Terms*—Power system restoration, high-impact low-probability (HILP) events, mixed-integer linear programming (MILP), wind energy, equipment vulnerability, resilience.**

NOMENCLATURE

A. Sets

$g \in \mathbf{G}$	Set of all generating units.
$i, j \in \mathbf{B}$	Set of transmission buses.
$d \in \mathbf{D}$	Set of load demands.
$k \in \mathbf{K}$	Set of transmission lines.
$t \in \mathbf{T}$	Set of restoration times.
$w \in \mathbf{W}$	Set of wind farms.
$\mathbf{G_{BS}}, \mathbf{G_{NBS}}$	Set of black-start and non-black-start generating units.
$\mathbf{B_{BS}}, \mathbf{B_{NBS}}$	Set of buses connected to the black-start and non-black-start generating unit g.
$\mathbf{B_k}, \mathbf{B_d}$	Set of buses connected to transmission line k and system load point d.
$\mathbf{K_i}, \mathbf{K_s}, \mathbf{K_r}$	Set of transmission lines connected to bus i, set of transmission lines with the sending end bus i and set of transmission lines with receiving end bus i.
$\mathbf{G_i}$	Set of generating units connected to bus i.
$\mathbf{D_i}$	Set of load demands at bus i.
$\mathbf{W_i}$	Set of wind farms connected to bus i.
$\mathbf{B_w}$	Set of buses connected to wind farms w.

B. Parameters and Constants

$P_g^{\max}, P_g^{\min}$	Maximum and minimum real power capacity of generating unit g.
$Q_g^{\max}, Q_g^{\min}$	Maximum and minimum reactive power capacity of generating unit g.
P_g^{start}	Cranking power of generating unit g.
$P_d^{\max}, P_d^{\min}$	Maximum and minimum restorable real load at load point d.
$Q_d^{\max}, Q_d^{\min}$	Maximum and minimum restorable reactive load at load point d.
$P_k^{\max}, P_k^{\min}$	Maximum and minimum real power limit of transmission line k.
$Q_k^{\max}, Q_k^{\min}$	Maximum and minimum reactive power limit of transmission line k.
δ_d	Priority factor of demand d.
T_s	Start-up duration of generating unit g.
RR_g	Ramp rate of generating unit g.
b_k	Series admittance of transmission line k.
b_{k0}	Shunt admittance of transmission line k.
g_k	Conductance of transmission line k.
η_g	Load pickup factor of generating unit g.
$P_{w,t}^{\text{fore}}, Q_{w,t}^{\text{fore}}$	Wind farm's forecasted real and reactive power at time t.

C. Decision Variables

$n_{g,t}$	Binary variable equal to 0/1 if generating unit g is off/on at time t.
$n_{g,t}^{\text{start}}$	Binary variable equal to 0/1 if generating unit g is out/in during the start-up period.
$n_{i(j),t}$	Binary variable equal to 0/1 if bus i or j is de-energized/energized at time t.
$n_{k,t}$	Binary variable equal to 0/1 if line k is de-energized/energized at time t.
$P_{d,t}, Q_{d,t}$	Amount of real and reactive restored load at the load point d at time t.
$P_{g,t}, Q_{g,t}$	Scheduled real and reactive power of generating unit g at time t.
$P_{g,t}^{\text{start}}$	Cranking power of generating unit g at time t.
$P_{k,t}, Q_{k,t}$	Real and reactive power flow in transmission line k at time t.
$V_{i(j),t}$	Bus voltage magnitude in p.u. at bus i or j at time t.
$\Delta V_{i(j),t}$	Bus voltage magnitude deviation from 1 p.u. at bus i or j at time t.
$\theta_{k,t}$	Phase angle difference across transmission line k at time t.
$n_{w,t}$	Binary variable equal to 0/1 if wind farm w is

978-1-7281-0407-2/19/$31.00©2019 IEEE

off/on at time t.

$P_{w,t}, Q_{w,t}$ Wind farm's scheduled real and reactive power at time t.

I. Introduction

Recently, a number of high-impact low-probability (HILP) incidents have threatened more frequently the security of the bulk electric power system. Whenever and wherever such incidents occur, there will be operation violations in the grid and possibly a large loss of electricity supply in the load points, which can potentially lead to a system-wide blackout [1]. According to recent reports, near 78% of the recorded electric grid disruptions between 1992 to 2012 were weather-related outages [2]–[5]. For instance, the Wenchuan earthquake in 2008 caused extreme damages in 966 substations, 274 transmission lines of multiple voltage levels and 1700 circuit lines [6], and the Hurricane Sandy in 2012 resulted in 10 percent of customers in New Jersey without power for 10 days which caused $14 billion to $26 billion economic losses [7]. Other than natural disasters, incidents caused by human activities also give birth to additional challenges in modern power grids. Operation errors in the grid resulted in the Northeast Blackout in 2003, which left more than 50 million people without power and caused $4 billion to $10 billion economic losses [8]. The cyber-attack on Ukrainian power grid in 2015 caused nearly 225,000 people without electricity for several hours [9], [10].

It is, therefore, urgently needed to design effective strategies for enhanced power system resilience following HILP events which can cause large system blackouts [11]. The black-start (BS) generating units are commonly utilized for system recovery following large-area, long-duration outages [1]. A BS is the process of restoring a part of or the entire electrical grid to normal operation without relying on energy transfer from the external electric power sources [12]. In [13], a recovery strategy is proposed to determine an optimal generator start-up sequence for BS restoration, while [14] applied a similar algorithm to determine an optimal transmission recovery path. Reference [15] coordinated the generation and load pickup processes to ensure power system reliability during the BS restoration. In [16], a new method is introduced which can optimize the start-up sequence and the associated restoration paths simultaneously. There are other mechanisms that can be employed for restoration, among which is the flexible use of tie lines (TLs) which can provide power system operators with different restoration decisions following a blackout [17].

With the increasing penetration of variable renewable energy resources, battery energy storage units are more widely used to improve power system resilience and reduce the restoration interval [11], [18]. In 2008, the department of energy (DOE) published a report indicating a goal of achieving 20% wind energy supply of the country's electricity by 2030 [19]. Reference [20] presented several aspects of power system restoration considering wind farms participation. In [21], a doubly fed induction generator (DFIG) based wind turbine can provide a strong contribution to a fast restoration during the BS process. Reference [22] proposed the application of permanent-magnet synchronous generator (PMSG) based wind turbines in BS procedures. The incorporation of wind power in a self-healing power grid can lead to a fast load outage recovery, thereby ensuring the grid resilience [18].

Most recent studies have been focusing on the development of restoration strategies with renewable energy resources, where the equipment and infrastructure damages are loosely incorporated. The vulnerability of power grid elements should be taken into account to achieve informative decisions that are in line with practical power system restoration planning. In this paper, a mixed-integer linear programming (MILP) model is presented to enhance the BS restoration capability using wind energy. The proposed model is applied to the IEEE 118-bus system test case in which multiple transmission lines are assumed offline due to a severe HILP incident.

The rest of this paper is organized as follows. Section II presents the general procedure of system restoration. Power system restoration formulation is presented in section III. The numerical results and discussions are provided in section IV, and finally section V concludes the paper.

II. Power Grid Restoration And Wind Energy

Following a large-area long-duration blackout, electric power system operators need to take a sequence of actions to return the system back to the normal operating condition. Power system restoration generally includes the following steps: black-start units (BSUs) start-up, transmission lines energization, non-black-start units (NBSUs) start-up, and load pickup [23]. Fig. 1 illustrates the general process of power system restoration. Before initiating a system restoration plan, power system operators need to check the status of system components and acquire the required data corresponding to the system initial condition. When the recovery plan is implemented, BSUs start quickly and provide the required energy to the transmission system. In the process of restoration, each transmission line is energized through a specific sequence based on the transmission network topology. Unlike BSUs which do not require external power from the adjacent grid to operate, NBSUs need to obtain cranking power for operation. As BSUs and transmission lines become energized, power is provided to start the NBSUs and satisfy the load demands. In order to recover the system swiftly, it is always critical to ensure and enhance the total generation capability in the network and minimize the load shading during the entire process of restoration.

Wind generators require extra control system to achieve a BS function. For instance, the storage system in DC link of a DFIG is used for BS in [22]. As a result, they are typically and here considered as NBSUs. Moreover, wind output power can highly fluctuate and causes large ramping rates [18] which enables wind power generators to supply the electricity faster than traditional power generation units. Thus, it may be advantageous to incorporate wind energy as a potentially promising energy resource into the power system restoration plans as illustrated in Fig 1.

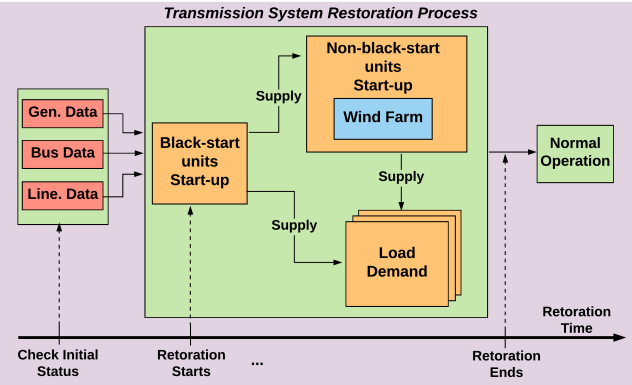

Fig. 1. Power system restoration process following a large scale blackout.

III. Problem Formulation

This section presents a MILP optimization model for power system restoration following a HILP-engendered blackout. The objective function includes three terms, as following:

$$\max(\sum_{t\in\mathbf{T}}\sum_{g\in\mathbf{G}}(P_g^{\max}-P_g^{\text{start}})n_{g,t}+\sum_{t\in\mathbf{T}}\sum_{w\in\mathbf{W}}P_{w,t}^{\text{fore}}n_{w,t} - \sum_{t\in\mathbf{T}}\sum_{d\in\mathbf{D}}\delta_d(P_d^{\max}-P_{d,t})) \tag{1}$$

The first and second terms indicate the total generation capability in the system including conventional generators and wind generators. The last term is the unserved load during the restoration which are served from high to low priority.

Several constraints should be taken into account including those corresponding to the initial conditions, energization sequence, components characteristics, power balance, and load pickup which are explained in the following.

A. Initial Conditions Constraints

In this paper, we assume that a large blackout have resulted in the total power system being de-energized. At the beginning of the restoration, none of the components in the system are energized, while they are physically not damaged and are all available to be online during the restoration. Constraints (2)-(6) imply that all generating units are off, and transmission buses and lines are de-energized. Constraint (7) illustrates that the BSUs start at $t=1$.

$$n_{g,t=0}^{\text{start}}=0,\quad g\in\mathbf{G} \tag{2}$$

$$n_{w,t=0}=0,\quad w\in\mathbf{W} \tag{3}$$

$$n_{g,t=0}=0,\quad g\in\mathbf{G} \tag{4}$$

$$n_{i(j),t=0}=0,\quad i,j\in\mathbf{B} \tag{5}$$

$$n_{k,t=0}=0,\quad k\in\mathbf{K} \tag{6}$$

$$n_{g,t=1}^{\text{start}}=1,\quad g\in\mathbf{G_{BS}} \tag{7}$$

B. Energization Sequence Constraints

Based on the transmission network topology, all system components are energized step by step. When the BSUs operate normally, the buses connected to them would be energized first and are represented in constraint (8). Since NBSUs require cranking power from external sources, they can operate only after the connected buses are energized (9). Constraint (10) denotes that generating unit g becomes available after the start-up period. Constraint (11) illustrates that wind farm unit w cannot operate until its connection bus is energized. Constraint (12) reflects that a transmission line is energized, only when any one of its connection buses is energized. If transmission line k is damaged, the value of $n_{w,t}$ will be 0 in the process of restoration. Constraint (13) illustrates that if a transmission line is energized at $t+1$, then at least one of the sending and receiving buses has been energized at time t. Constraint (14) shows that a bus connected to NBSUs is energized, when any transmission lines connected to that bus are energized. Constraints (15) and (16) present that once a bus or transmission line is energized, it will not be de-energized again.

$$n_{g,t}\geq n_{i,t},\quad g\in\mathbf{G_{BS}},i\in\mathbf{B_{BS}} \tag{8}$$

$$n_{g,t}^{\text{start}}\leq n_{i,t},\quad g\in\mathbf{G_{NBS}},i\in\mathbf{B_{NBS}} \tag{9}$$

$$n_{g,t+T_s}\leq n_{g,t}^{\text{start}},\quad g\in\mathbf{G} \tag{10}$$

$$n_{w,t}\leq n_{i,t},\quad i\in\mathbf{B_w} \tag{11}$$

$$n_{k,t}\leq n_{i(j),t},\quad i,j\in\mathbf{B_k} \tag{12}$$

$$n_{k,t+1}\leq n_{i,t}+n_{j,t},\quad i,j\in\mathbf{B_k} \tag{13}$$

$$n_{i,t}\leq\sum_{k\in\mathbf{K_i}}n_{k,t},\quad i\in\mathbf{B_{NBS}} \tag{14}$$

$$n_{i,t}\leq n_{i,t+1},\quad i\in\mathbf{B} \tag{15}$$

$$n_{k,t}\leq n_{k,t+1},\quad k\in\mathbf{K} \tag{16}$$

C. Components Characteristics Constraints

Constraints (17) and (18) enforce the minimum and maximum limits on the real and reactive output power of generating unit g. The output power of each generator is limited by its ramping rate, as shown in constraint (19). Similarly, constraints (20) and (21) illustrate the real and reactive power flow limitations of transmission lines, while constraints (22) and (23) present the limits on the real and reactive loads. Constraint (24) denotes the required cranking power for generating unit g at time t. The scheduled power of a wind farm should be limited within its boundary, as stated in (25) and (26).

$$P_g^{\min}n_{g,t}\leq P_{g,t}\leq P_g^{\max}n_{g,t} \tag{17}$$

$$Q_g^{\min}n_{g,t}\leq Q_{g,t}\leq Q_g^{\max}n_{g,t} \tag{18}$$

$$-RR_g\leq P_{g,t+1}-P_{g,t}\leq RR_g \tag{19}$$

$$P_k^{\min}n_{k,t}\leq P_{k,t}\leq P_k^{\max}n_{k,t} \tag{20}$$

$$Q_k^{\min}n_{k,t}\leq Q_{k,t}\leq Q_k^{\max}n_{k,t} \tag{21}$$

$$P_d^{\min}n_{i,t}\leq P_{d,t}\leq P_d^{\max}n_{i,t},\quad i\in\mathbf{B_d} \tag{22}$$

$$Q_d^{\min}n_{i,t}\leq Q_{d,t}\leq Q_d^{\max}n_{i,t},\quad i\in\mathbf{B_d} \tag{23}$$

$$P_{g,t}^{\text{start}}=P_g^{\text{start}}(n_{g,t}^{\text{start}}-n_{g,t}) \tag{24}$$

$$0\cdot n_{w,t}\leq P_{w,t}\leq P_{w,t}^{\text{fore}}n_{w,t} \tag{25}$$

$$0\cdot n_{w,t}\leq Q_{w,t}\leq Q_{w,t}^{\text{fore}}n_{w,t} \tag{26}$$

D. Power Balance Constraints

Real and reactive power should be balanced between generation and load, as shown in constraints (27) and (28). Inspired by [24], we utilized a linearized AC power flow model to obtain the real and reactive power flow of transmission lines, as reflected in constraints (29) and (30).

$$\sum_{g\in\mathbf{G_i}}(P_{g,t}-P_{g,t}^{\text{start}})+\sum_{w\in\mathbf{W_i}}P_{w,t}-\sum_{d\in\mathbf{D_i}}P_{d,t}=\sum_{k\in\mathbf{K_s}}P_{k,t}-\sum_{k\in\mathbf{K_r}}P_{k,t} \tag{27}$$

$$\sum_{g\in\mathbf{G_i}}Q_{g,t}+\sum_{w\in\mathbf{W_i}}Q_{w,t}-\sum_{d\in\mathbf{D_i}}Q_{d,t}=\sum_{k\in\mathbf{K_s}}Q_{k,t}-\sum_{k\in\mathbf{K_r}}Q_{k,t} \tag{28}$$

$$P_{k,t}=(\Delta V_{i,t}-\Delta V_{j,t})g_k-b_k\theta_{k,t} \tag{29}$$

$$Q_{k,t}=-(1+2\Delta V_{i,t})b_{k0}-(\Delta V_{i,t}-\Delta V_{j,t})b_k-g_k\theta_{k,t} \tag{30}$$

E. Load Pickup Constraints

During the restoration process, the amount of dynamic reserve should be considered to allow the system to restore within a safe range of frequency (i.e. 57.5Hz). The "load pickup factors" η_g can determine the amount of dynamic reserve during the restoration process [25]. The values of these factors is assumed to be the weighted total of 5% of the generation capacities in steam turbines, 15% of the generation capacities in hydro generators, and 25% of the capabilities in combustion turbines. Load pickup constraints are shown in (31) and (32), which can help maintain the system frequency in a safe margin during the restoration period.

$$\sum_{d\in\mathbf{D}}P_{d,t+1}-\sum_{d\in\mathbf{D}}P_{d,t}\leq\sum_{g\in\mathbf{G}}\eta_g P_{g,t} \tag{31}$$

$$P_{d,t+1}-P_{d,t}\geq 0 \tag{32}$$

IV. Numerical Results and Discussions

A. Test System Description

In this section, the modified IEEE 118-bus test system is employed as a case study to verify the efficiency of the proposed model. As shown in Fig. 2, the test system includes 19 generating units, 118 buses, and 185 transmission lines. The total amount of de-energized load following a severe HILP blackout is 4519 MW. The characteristics and data on system generators, buses and transmission lines are taken from [26]. We assumed that 3 generators g_3, g_6 and g_{19} are BSUs and the rest are NBSUs. There are three wind farms connected to bus 1, bus 19 and bus 74 with the total installed capacity of 600 MW, representing 13% penetration. All wind farms are operating at a unity power factor. In all cases, the base power is assumed to be 100 MW and each restoration time step is 10 minutes. The total period of restoration process is considered 4 hours. All simulations have been done on a PC with an Intel Xeon E5-2620 v2 processor and 16 GB of memory using Cplex 12.5.1. The following four cases are discussed to verify the impact of wind participation and transmission line damages on the restoration efficiency.

TABLE I
Generators' Optimal on Time and Types

Gen. No.	Time (min)	Turbine Type	Gen. No.	Time (min)	Turbine Type
g_1	220	Steam	g_{11}	170	Steam
g_2	110	Combustion	g_{12}	160	Steam
g_3	20	Hydro	g_{13}	160	Steam
g_4	80	Combustion	g_{14}	180	Steam
g_5	120	Combustion	g_{15}	120	Combustion
g_6	20	Hydro	g_{16}	80	Combustion
g_7	90	Combustion	g_{17}	100	Combustion
g_8	70	Combustion	g_{18}	60	Combustion
g_9	100	Combustion	g_{19}	20	Hydro
g_{10}	90	Combustion			

*1) **Case I**:* Which is the base case scenario with no wind farms participating in the restoration process and no transmission lines are damaged.

*2) **Case II**:* Wind farms participation in the restoration procedure and no transmission lines being damaged.

*3) **Case III**:* Wind farms are excluded from the proposed restoration plan, but some transmission lines are damaged.

*4) **Case IV**:* Both wind farms and transmission lines damages are included in the restoration process.

B. Numerical Results

1) Base Case Results: With the suggested optimization formulation, the total restored load in the system is achieved 4519 MW in *Case I*. Table I presents the optimal solutions when the conventional generating units are restored and become online in *Case I*. The BSUs g_1, g_6 and g_{19} become online at $t = 20$ minutes and the first NBSU g_{18} becomes online at $t = 60$ minutes. At $t = 220$, all generating units become fully available and functional. According to Fig. 3, the first load point is energized at $t = 20$ minutes when the load pickup process is initiated. Besides, it takes 180 minutes to recover all the total demanded load of the system following the simulated HILP event scenario.

2) Impact of Wind Participation: In *Case II*, three different wind farms are installed at bus 1, bus 19 and bus 74. The total capacity of wind farms is 600 MW. Fig. 4 depicts the total load pick up curves considering the wind farm participation in the restoration process. Compared with the base case scenario, the wind farms participation has increased the total load pickup at each restoration time step. For instance, at $t = 140$ minutes, the total restored load is 2907 MW in the base case scenario, while the total restored load is improved to 3217 MW considering the wind farms participation in the system.

3) Impact of Line Damages: In *Case III*, where several transmission lines are assumed damaged and out of service, the system is restored without wind participation. The damaged transmission lines are line 68, 69, 73, 76, 78, 79, 80, 81 and 82, as shown in Fig. 2 in red. In this case, the total restored load is 4463 MW, which is 98% of the total load demands in the system. According to Fig. 5, the system restoration performance in *Case I* is better than that in the *Case III*. Comparing the two test cases, it is obvious that less load is restored in *Case III* at each restoration time step. To put a

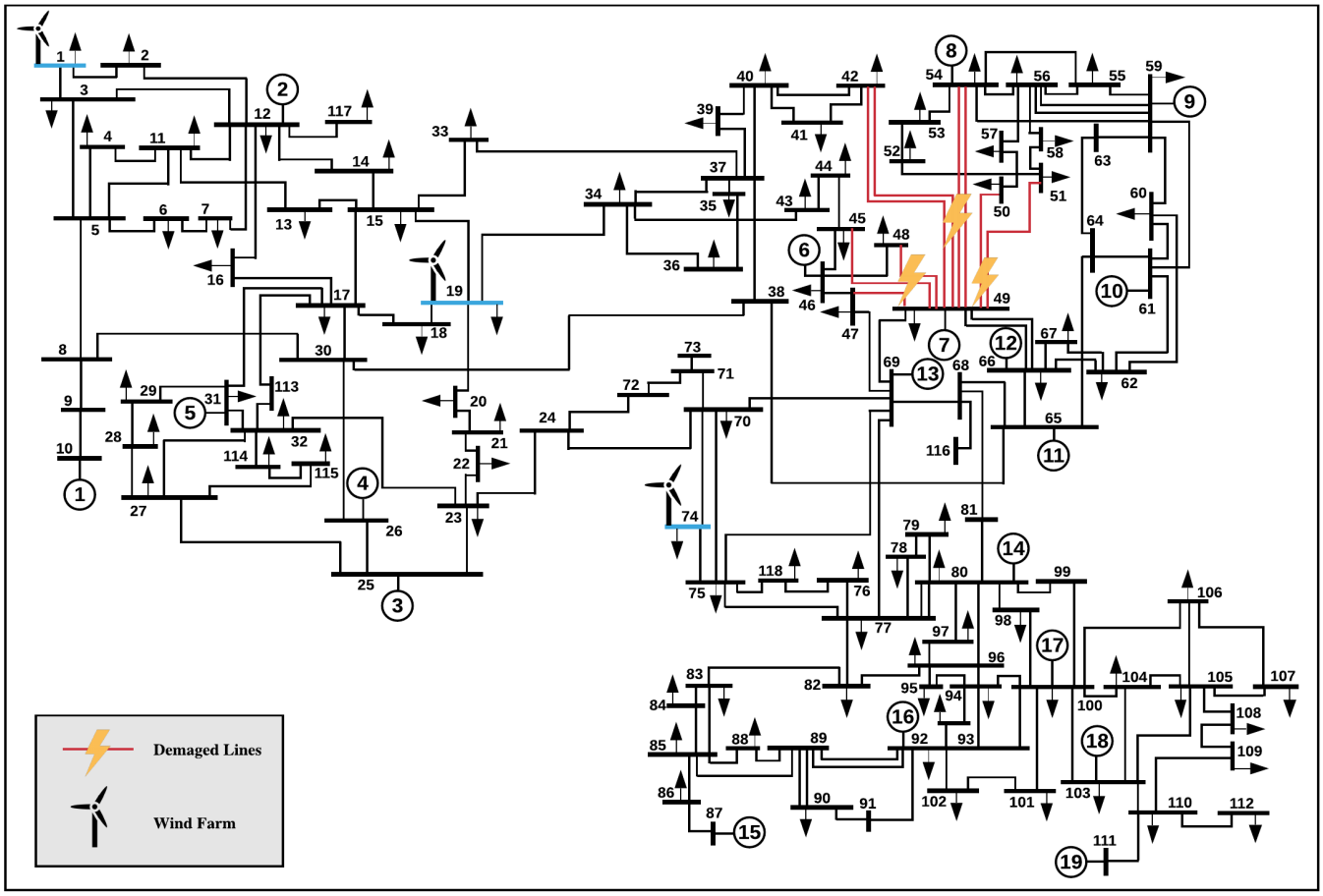

Fig. 2. The modified IEEE 118-bus test system.

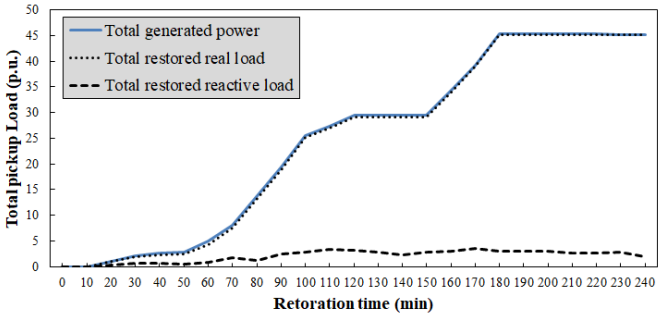

Fig. 3. Total generated power and load pickup in *Case I*.

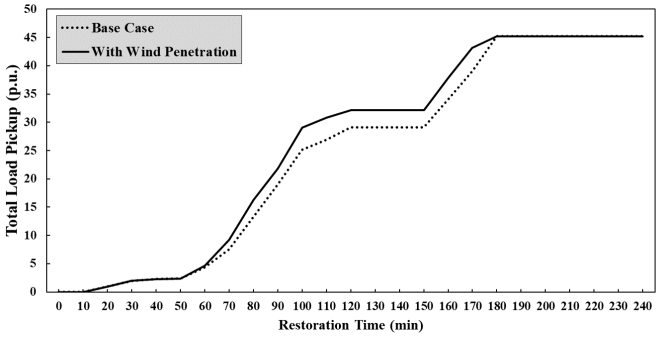

Fig. 4. Total load pickup with 600MW wind farms in *Case II*.

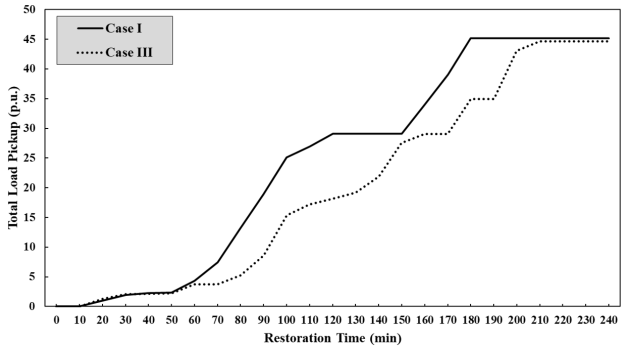

Fig. 5. Total load pickup in *Case I* and *Case III*.

figure on this, take $t = 140$ minutes as an examples, where 2907 MW load can be restored in *Case I*, while only 2185 MW load can be restored in *Case III*. In addition, due to the power flow limits of transmission lines, there are not enough power flow reaching the load points 42 and 50, and these load demands cannot be fully supplied. This implies that the system cannot be completely restored in this studied test case.

4) Impact of Wind Participation with Line Damages: In *Case IV*, the damaged lines are considered the same as those in *Case III*. We here utilized wind farms with total installed capacity of 600 MW to help in system restoration. The location of wind farms is the same as that in *Case II*. Fig. 6 illustrates the total load pickup with wind participation in *Case IV*. Compared with *Case III*, the total restored load of the system is

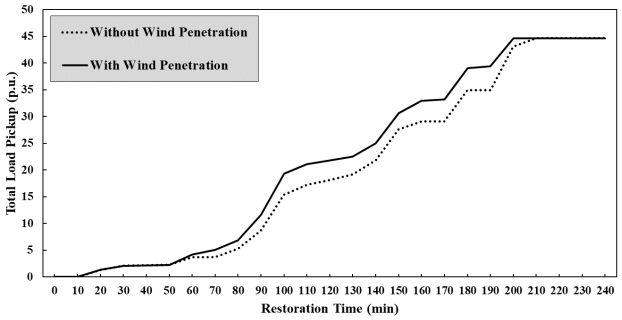

Fig. 6. Total load pickup with with 600MW wind farms in *Case IV*.

TABLE II
OPTIMAL RESTORATION TIME INCLUDING DIFFERENT WIND POWER PENETRATION LEVELS

Wind Penetration	*Case II* **Time (min)**	*Case IV* **Time (min)**
0%	180	210
13%	180	200
20%	170	200
27%	170	200

still 4463 MW, which can be achieved quickly through utilizing wind farms. Hence, although the system cannot be fully recovered in this case, wind participation in the restoration process can improve the system restoration capability, swift response and recovery, and an enhanced overall resilience.

5) Sensitivity Analysis of Different Wind Penetration Levels: We assume the wind power penetration in the system to be 13% (200MW) in *Case II* and *Case IV*. Table II illustrates the impact of different wind penetration levels on the system restoration period following a large-scale blackout. As it can be seen, the higher wind penetration in the system, the faster the system restoration. However, the network topology enforced a minimum cost of time required for a full restoration, and thus, the restoration time is the same for 20% and 27% wind penetration (shown in Table II). Moreover, increasing wind farms capacity comes at a significant expense, thereby calling for effective trade-off between investment costs and the system restoration agility.

V. CONCLUSION

In this paper, we developed a restoration planning mechanism to achieve an enhanced power system resilience following a blackout. The proposed method is formulated as a MILP optimization model and implemented on the IEEE 118-bus test system. The vulnerability of power grid elements following a HILP event is also modeled to verify the efficiency of the proposed restoration solution. Extensive numerical results clearly highlight that including wind power into the power system restoration processes can significantly improve the power grid response in terms of the total load restoration as well as the restoration agility, altogether enhancing the grid resilience in the face of HILP disasters and other outage-inducing patterns which potentially put the grid operation at risk to cascades and system blackouts. Future research could employ stochastic or robust optimization to discuss the impact of uncertain wind on system restoration.

REFERENCES

[1] E. National Academies of Sciences, Medicine, *et al.*, "Enhancing the resilience of the nations electricity system. 2017."

[2] E. Mills, "Electric grid disruptions and extreme weather," *Lawrence Berkeley National Laboratory*, 2012.

[3] R. J. Campbell, "Weather-related power outages and electric system resiliency," Congressional Research Service, Library of Congress Washington, DC, 2012.

[4] A. Kenward and U. Raja, "Blackout: Extreme weather climate change and power outages," *Climate central*, vol. 10, 2014.

[5] P. Dehghanian, B. Zhang, T. Dokic, and M. Kezunovic, "Predictive risk analytics for weather-resilient operation of electric power systems," *IEEE Trans. on Sustainable Energy*, vol. 10, no. 1, pp. 3–15, 2019.

[6] J. Eidinger, "Wenchuan earthquake impact to power systems," in *Lifeline Earthquake Engineering in a Multihazard Environment*, pp. 1–12, 2009.

[7] *Economic Benefits of Increasing Electric Grid Resilience to Weather Outages*. Executive Office of the President. Council of Economic Advisers, 2013.

[8] P. Dehghanian, S. Aslan, and P. Dehghanian, "Maintaining electric system safety through an enhanced network resilience," *IEEE Transactions on Industry Applications*, vol. 54, no. 5, pp. 4927–4937, Sept.-Oct. 2018.

[9] "Analysis of the cyber attack on the ukrainian power grid," *Electricity Information Sharing and Analysis Center (E-ISAC)*, 2016.

[10] S. Wang, P. Dehghanian, M. Alhazmi, and M. Nazemi, "Advanced control solutions for enhanced resilience of modern power-electronic-interfaced distribution systems," *Journal of Modern Power Systems and Clean Energy*, pp. 1–15, 2019.

[11] M. Nazemi and *et al*., "Energy storage planning for enhanced resilience of power distribution networks against earthquakes," *IEEE Transactions on Sustainable Energy*, 2019.

[12] U. G. Knight and U. Knight, *Power systems in emergencies: From contingency planning to crisis management*, vol. 2. John Wiley, 2001.

[13] W. Sun, C.-C. Liu, and L. Zhang, "Optimal generator start-up strategy for bulk power system restoration," *IEEE Transactions on Power Systems*, vol. 26, no. 3, pp. 1357–1366, 2010.

[14] W. Sun and C.-C. Liu, "Optimal transmission path search in power system restoration," in *2013 IREP Symposium Bulk Power System Dynamics and Control-IX Optimization, Security and Control of the Emerging Power Grid*, pp. 1–5, IEEE, 2013.

[15] Z. Qin, Y. Hou, C.-C. Liu, S. Liu, and W. Sun, "Coordinating generation and load pickup during load restoration with discrete load increments and reserve constraints," *IET Generation, Transmission & Distribution*, vol. 9, no. 15, pp. 2437–2446, 2015.

[16] Z. Hainan, W. Yan, W. Juanjuan, L. Kun, L. Xiaohui, W. Xuesong, Z. Fan, Y. Na, and X. Richang, "Multi-objective preference optimization of unit restoration during network reconstruction based on de-eda," in *2018 China International Conference on Electricity Distribution (CICED)*, pp. 1327–1333, IEEE, 2018.

[17] A. Stefanov, C.-C. Liu, M. Sforna, M. Eremia, and R. Balaurescu, "Decision support for restoration of interconnected power systems using tie lines," *IET Generation, Transmission & Distribution*, vol. 9, no. 11, pp. 1006–1018, 2015.

[18] A. Golshani, W. Sun, Q. Zhou, Q. P. Zheng, and Y. Hou, "Incorporating wind energy in power system restoration planning," *IEEE Transactions on Smart Grid*, 2017.

[19] N. None, "20% wind energy by 2030: Increasing wind energy's contribution to us electricity supply," tech. rep., EERE Publication and Product Library, Washington, DC (United States), 2008.

[20] H. Zhu and Y. Liu, "Aspects of power system restoration considering wind farms," 2012.

[21] M. Aktarujjaman, M. Kashem, M. Negnevitsky, and G. Ledwich, "Black start with dfig based distributed generation after major emergencies," in *2006 International Conference on Power Electronic, Drives and Energy Systems*, pp. 1–6, IEEE, 2006.

[22] Y. Tang, J. Dai, Q. Wang, and Y. Feng, "Frequency control strategy for black starts via pmsg-based wind power generation," *Energies*, vol. 10, no. 3, p. 358, 2017.

[23] M. Adibi, "Power system restoration," *Methodologies and Implementation Strategies. IEEE Series on Power Engineering*, 2000.

[24] H. Zhang, G. T. Heydt, V. Vittal, and J. Quintero, "An improved network model for transmission expansion planning considering reactive power and network losses," *IEEE Transactions on Power Systems*, vol. 28, no. 3, pp. 3471–3479, 2013.

[25] P. Manual, "36: System restoration," *PJM: Valley Forge, PA, USA*, 2013.

[26] P. Dehghanian, *Power System Topology Control for Enhanced Resilience of Smart Electricity Grids*. PhD thesis, Texas A&M University, 2017.